COMPETITION BETWEEN NEUTRON AND CHARGED PARTICLE EMISSION FROM COMPOUND NUCLEI AROUND A = 160

R. Kossakowski, J. Jastrzębski, Z. Preibisz, P. Rymuza and W. Skulski
Institute of Nuclear Research, 05-400 Swierk, Poland

S. André, J. Genevey, A. Gizon, J. Gizon and V. Barci
Institut des Sciences Nucléaires, IN2P3, USMG, 38026 Grenoble-Cedex, France.

Abstract

Cross sections of reaction products from the interaction of 5-10 MeV/nucleon ^{12}C, ^{14}N and ^{16}O ions with targets of mass around A=150 are investigated using gamma ray detection techniques. The competition between various reaction channels in which from 0 to 4 charges are removed from the compound nucleus is studied as a function of excitation energy of the compound nucleus (CN) and of the distance of the CN from the stability line. The experimental data are compared with the predictions of the evaporation model using the ALICE code.

1. Introduction

The principal limitation for the production of very neutron deficient nuclei in heavy ion reactions is due to the increasing probability of charged particle emission when either the excitation energy of the compound nucleus, or its distance from the stability line, increase. Although qualitative features of the competition between neutron and charged particle emission are quite well understood, there is a very limited amount of quantitative experimental data. This competition was previously investigated by Stephens et al.[1]. In this work an effective proton binding energy including the Coulomb barrier was determined in a number of reactions and a simple relationship between proton to neutron evaporation rates, binding energies and nuclear temperature was established. More complete evaporation calculations were performed by Winn et al.[2].

In the present work we investigate the production cross sections of final nuclei, observed in light-heavy ion induced reactions on a number of targets with mass around A = 150. Gamma ray techniques were employed. The compound systems formed in these reactions span a large region of nuclei in respect to the stability line. Varying projectile energies, we were able to deduce the relative importance of the charged particle emission (as compared to the neutron emission alone) as a function of excitation energy of the compound nucleus (CN) and the distance of the CN from the stability line. Some part of the data presented in this communication has been published before[3].

2. Experimental method

The ^{141}Pr, ^{144}Sm, ^{147}Sm, ^{150}Sm, ^{152}Sm and ^{154}Sm targets, 10-20 mg/cm^2 thick, were irradiated with ^{12}C and ^{14}N ions and ^{141}Pr target also with ^{16}O ions from the variable energy cyclotron at ISN, Grenoble. The incident energy was varied between 71 MeV and 110 MeV for ^{12}C ions, between 68 MeV and 145 MeV for ^{14}N ions and between 100 MeV and 130 MeV for ^{16}O ions. Only part of the collected data has been evaluated so far.

The gamma rays were detected with a 10-15% efficiency Ge(Li) detector, placed at 55° in respect to the beam axis at a distance of about 10 cm from the target. The gamma ray spectra were measured in coincidence with the beam burst,

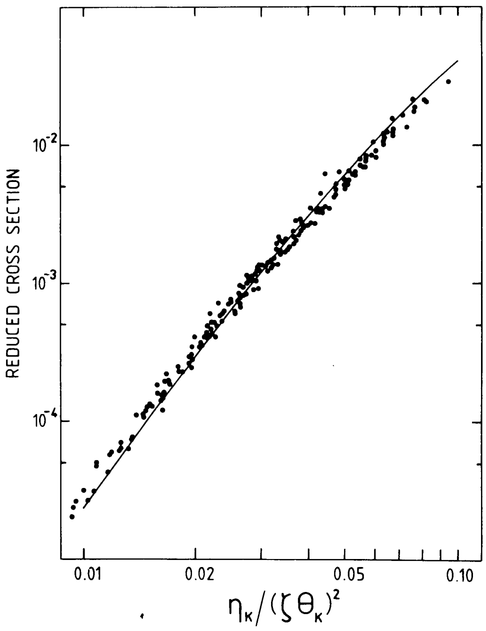

Fig. 1 K-shell ionization cross section for target elements with $37 \leqslant Z \leqslant 57$ and ^{12}C, ^{14}N and ^{16}O projectiles in an universal representation. The abscissa represents the scaled projectile velocity and the ordinate the reduced cross section. The experimental cross sections of Refs. 8, 9 are corrected for polarization in conjunction with the binding effect[11], relativistic effect[12] and Coulomb deflection[13]. The continuous line is the $F_K(\eta_K/(\zeta\theta_K)^2)$ function calculated from the PWBA and tabulated in Ref. 10. The energies of ions from the present work correspond to $\eta_K/(\zeta\theta_K)^2$ between 0.05 and 0.10. See Refs. 10, 11 for the meaning of symbols used in this figure.

	81	82	83	84	85	86	87	88
Er 68		150 ~45	151 82	152 30	153	154	155	156 C.N.
Ho 67		149 5	150 ~91	151 260	152 106	153	154	155
Dy 66	147 ~30	148 124	149 124	150 104	151 35	152	153	154
Tb 65	146 $\leqslant 9$	147 37	148 84	149 69	150			
Gd 64	145 25	146 63	147 38	148 25				

$^{12}C + ^{144}Sm$, $E^* = 76$ MeV

$\Delta E^* = 14$ MeV

Fig. 2 Distribution of the cross section for the $^{12}C + ^{144}Sm$ reaction at 110 MeV bombarding energy (103 MeV mean energy at the half thickness of the target). The cross sections are given in mb. The relative errors are between 10% and 20% for values exceeding 30 mb.

between bursts, and immediately after the beam shut-off.

For a given target-projectile-energy combination the relative cross sections for the production of final nuclei were deduced basing on in-beam transition intensities leading to the ground or low lying states of these nuclei as well as from radioactive transitions (corrected for recoils) measured between beam bursts and after the beam shut-off. The energies and branching ratios of the radioactive gamma transitions were taken mainly from Ref. 4. The available literature data on the in-beam transitions were catalogued in order to facilitate the atributions.

The excitation functions and absolute cross sections were obtained using the target K X-rays measured simultaneously with the gamma rays in each run. This normalization method was previously employed for lighter ions[5,6], where the K-shell ionization cross sections are relatively well known or may be reliably calculated[7]. In order to test whether the calculations may give reliable K-shell ionization cross sections for heavier projectiles the available experimental data from Refs. [8], 9 were compared with the calculated cross sections obtained from the plane-wave Born approximation[10] (PWBA) with a number of corrections[11-13]. Fig. 1 shows these data in an universal representation in which the reduced cross sections are plotted against the reduced bombarding energy and compared with calculations. The experimental data exist for projectiles of a similar atomic number as employed in the present work but for slightly lighter targets. Although the calculated curve deviates slightly (up to 20%) from the experimental data, at the present stage we use the calculated K-shell ionization cross sections for normalization purposes.

3. Results

From the experiment we determined the distribution of the cross section among almost all the residual nuclei with $\sigma \gtrsim 10$ mb. Fig. 2 shows an example of such a distribution in the $^{12}C + ^{144}Sm$ reaction at 110 MeV incident energy. The compound nucleus, ^{156}Er, is the farest from the

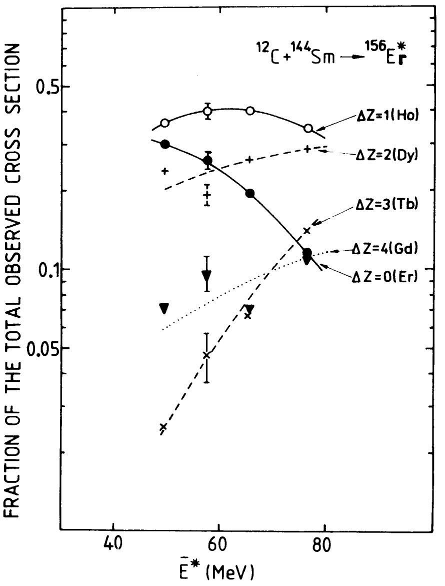

Fig. 3 Fraction of the total observed cross section for different values of the removed charge (isotopic yield) as a function of excitation energy of the compound nucleus ^{156}Er.

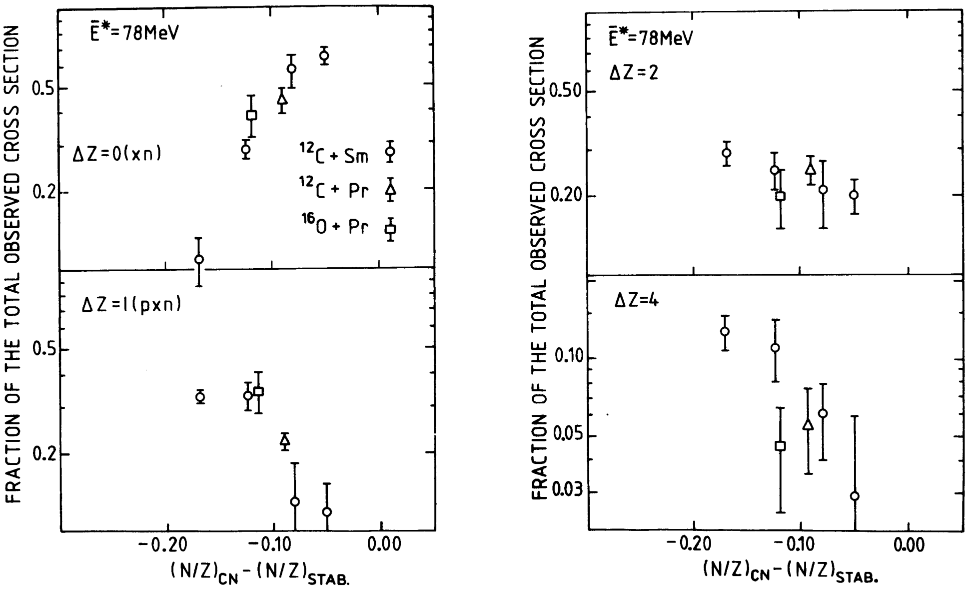

Fig. 4 Fraction of the total observed cross section for different values of the removed charge as a function of the distance of the compound nucleus from the stability line. Data points, for a fixed excitation energy (78MeV), were obtained from the interpolation of results similar to those, shown in Fig. 3. The N/Z of the stability line is obtained from the abundance weighted N/Z values of stable, even-even nuclei.

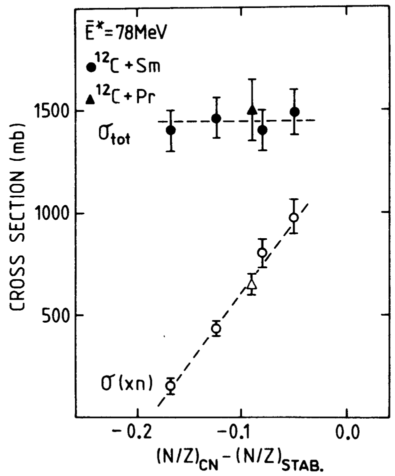

Fig. 5 Absolute values of the total observed cross section and of the (HI, xn) channel cross section as a function of the distance of the compound nucleus from the stability line for E* = 78MeV.

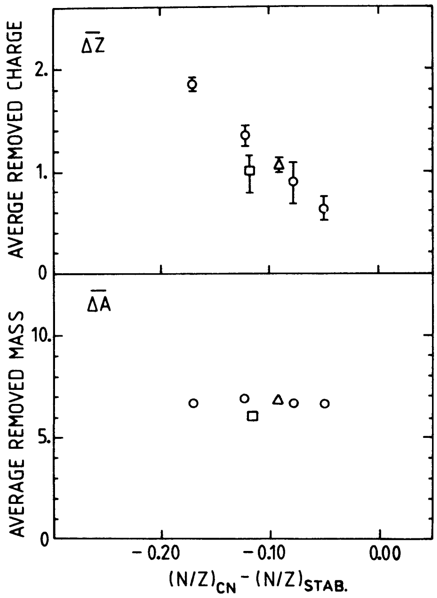

Fig. 6 Average removed charge and average removed mass as a function of the distance of the compound nucleus from the stability line for E* = 78MeV. The error bars of the $\overline{\Delta A}$ values are smaller than data points.

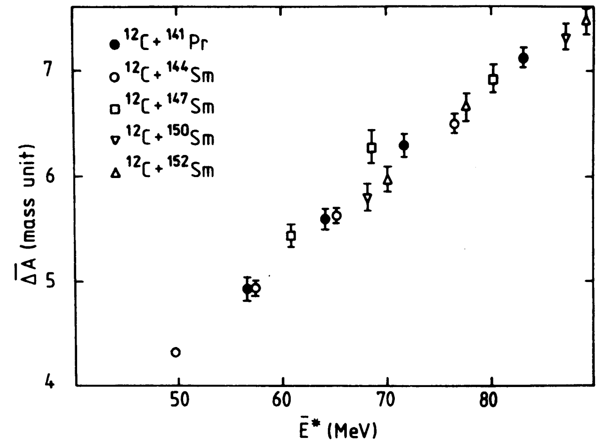

Fig. 7 Average removed mass as a function of the excitation energy of the compound nucleus.

stability line (among systems investigated in this work). The total observed cross section of 1379mb is distributed here among 19 final products.

The relative contribution to the total observed cross section of various reaction channels in which from 0 to 4 charges were removed from the CN (isotopic yield) is shown in Fig. 3. From similar data the relative contribution of various channels was deduced as a function of the distance of the compound nucleus from the stability line and is shown in Fig. 4. It is seen that for the excitation energy of 78MeV about 70% of the observed cross section goes into (HI,xn) products in case of ^{164}Er*, whereas this fraction drops to 10% for the ^{156}Er* compound nucleus.

The absolute values of the total observed cross sections and of the (HI,xn) channel cross section are shown in Fig. 5 for the 78MeV excitation energy. We see that at this excitation energy the (HI,xn) channel would have a negligible cross section for a compound nucleus with N/Z difference of -0.18 (e.g. ^{154}Er).

The average values of the removed charge ($\overline{\Delta Z}$) and mass ($\overline{\Delta A}$) for the same excitation energy are presented in Fig. 6. The extrapolation of the experimental data suggests that even at this rather high excitation energy the $\overline{\Delta Z}$ value should be close to zero at the stability line. This may indicate that the incomplete fusion mechanism 14) is of no major importance in the energy range studied in the present work. (However, see also the following section).

Finally, in Fig. 7 the average removed mass is presented as a function of the excitation energy of the compound nucleus. The slope of a straight line fitted to the data points of Fig. 7 is (12.6 ± 0.7) MeV/mass unit. No deviation from a straight line, which would indicate a substantial emission of fast particles, is discernable within the experimental errors.

4. Discussion

The experimental data of the previous section were compared with the evaporation model using the code ALICE 15). The calculations were performed using Myers-Swiątecki Lysekil liquid drop masses with no paring and no shell correction. The s-wave approximation with a liquid drop moment of inertia was chosen. The absolute values of the calculated cross section were normalized to the observed cross section using a multiplicative factor which was close to 0.8.

The comparison of the experimental data with the evaporation calculations is shown in Figs. 8-10. It is seen that the ratios of the calculated over the experimental values of the cross section and of the average values ($\overline{\Delta Z}$ and $\overline{\Delta A}$) change smoothly both as a function of excitation energy and of the distance from the stability line. The calculated average evaporated mass is systematically about 10% lower than the $\overline{\Delta A}$ of Fig. 7 in the whole energy range. For all but ^{156}Er compound nuclei the code seriously underestimates all channels with charged particle emission in comparison with the (HI,xn) channel. (In the ^{156}Er case only $\Delta Z = 4$ channel is strongly depressed in the calculation). It was thought that a part of this discrepancy, at least for the $\Delta Z = 2$ and $\Delta Z = 4$ channels, may perhaps be accounted for by the presence of other than complete fusion processes. In order to investigate this possibility the calculation was performed 16) using the "Sum Rule Model" of Wilczyński et al. 17) with the same parameters as in Ref. 17. At the highest energies

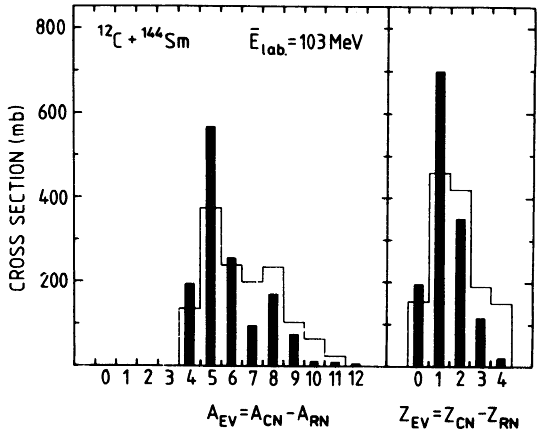

Fig. 8 Comparison of the observed mass and charge distribution of the reaction products from the ^{12}C + ^{144}Sm reaction with predictions of the evaporation model. The experimental data (open rectangles) are deduced from Fig. 2. Calculated cross sections (solid bars) are obtained with the code ALICE, with parameters described in the text and after the normalization of the total calculated cross section to the total observed cross section. The energy spread in the target is taken into account in the calculation.

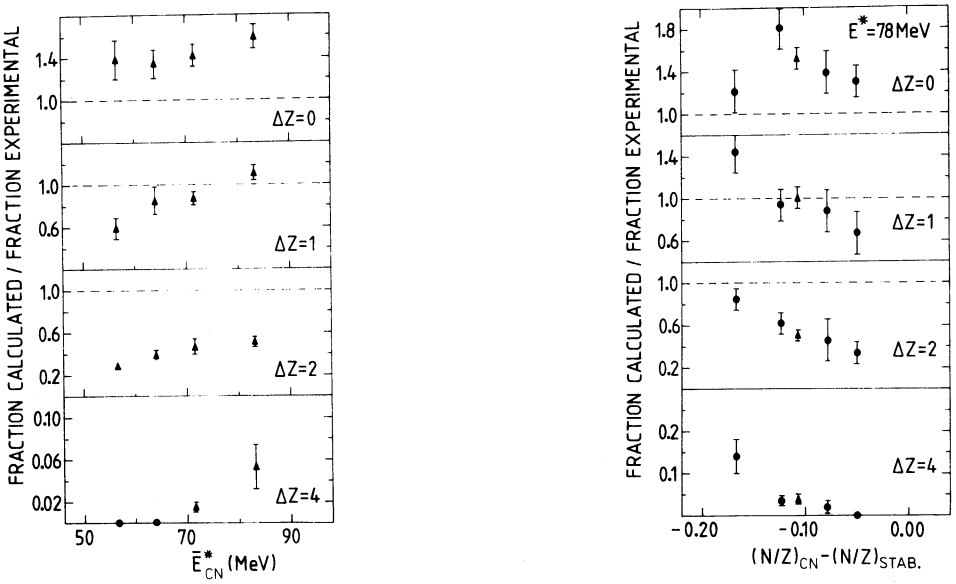

Fig. 9. Comparison of the isotopic yields as a function of the excitation energy (for the ^{12}C + ^{141}Pr reaction) and distance from the stability line (for E* = 78 MeV, experimental data of fig. 4) with the predictions of the evaporation model. The error bars are only from the experimental data. See also caption to Fig. 8.

employed in this work the calculated cross section for the emission of fast α particles (the strongest non-equilibrium channel) was as high as 1/3 of the observed cross section for the ΔZ = 2 products. However, the model does not account for the substantial cross section of the ΔZ = 1 and ΔZ = 4 products and for the relatively slow variation of the cross section of the ΔZ = 2 products with the incident energy.

Therefore, taking into account the results discussed in connection with Figs. 6 and 7, we conclude that the ALICE code underestimates the reaction channels in which one or more charged particle is removed from the compound nucleus. However, in view of the ^{156}Er result, this conclusion may be not valid very far from the stability line.

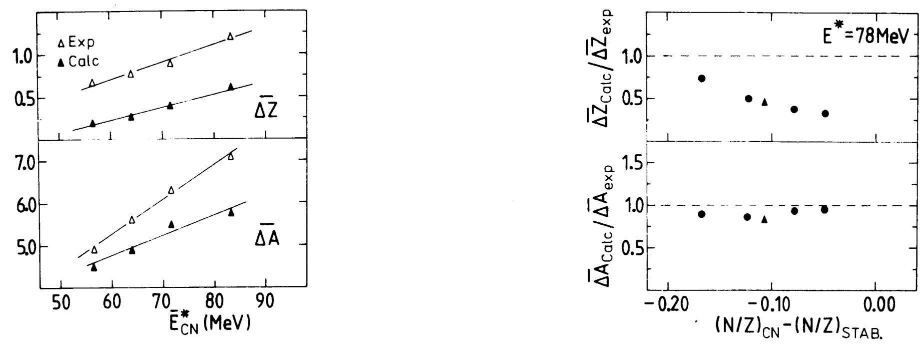

Fig. 10. Comparison of the average removed mass and charge as a function of the excitation energy (for the ^{12}C + ^{141}Pr reaction) and distance from the stability line (for E* = 78 MeV, experimental data of Fig. 6) with the predictions of the evaporation model. See also caption to Fig. 8.

5. Summary and conclusions

Employing the gamma ray detection techniques we were able to determine the distributions of the cross section among all the residual nuclei with $\sigma \geq 10$ mb for many target-projectile-incident energy combinations. These data allow us to follow in a quantitative way the competition between various reaction channels in which from 0 to 4 charges are removed from the compound nuclei of different excitation energy or different distance from the stability line. It was shown that, for a fixed excitation energy of the compound nucleus, the cross section of the (HI,xn) channel and the average removed charge change linearly with the distance of the compound nucleus from the stability line. Within the energy range investigated in this work, the average removed mass also exhibits almost linear dependence on the excitation energy of the compound nucleus and is independent of the position of the compound nucleus in respect to the stability line.

The evaporation calculations performed with the code ALICE show a moderate agreement with the experimental data. With the options used in this work the code underestimates the reaction channels with charged particle emission in comparison with the (HI,xn) channel. Only part of this effect may be attributed to the presence of the incomplete fusion reactions.

We are indebted to Dr H. Karwowski, Dr J. Łukasiak and Dr J. Wilczyński for helpful discussions. We also thank Mr G. Margotton, Dr M. Moszyński and Mr P. Richaud for technical assistance in many stages of this work. This work has been carried out within the Grenoble - Świerk collaboration, operating under IN2P3 - Warsaw University agreement.

References

1. F.S. Stephens, J.R. Leigh and R.M. Diamond Nucl. Phys. A170 (1971) 321.
2. W.G. Winn, H.H. Gutbrod and M. Blann, Nucl. Phys. A188 (1972) 423.
3. The Grenoble - Swierk Collab., Proc. Conf. on Large Amplitude Collective Motions (Keszthely, 1979) p. 71; Proc. Intern. Conf. on Nuclear Behaviour at High Angular Momentum (Strasbourg, 1980) p. 59; Phys. Letters 97 B (1980) 50.
4. U. Reus, W. Westmeier and I. Warnecke, GSI-Rep. 79-2.
5. J. Kropp et al., Z. Phys. A280 (1977) 61.
6. D. Chmielewska et al., Nukleonika 23 (1978) 333.
7. J.D. Garcia, R.J. Fortner and T.M. Kavanagh Rev. Mod. Phys. 45 (1973) 111.
8. R.K. Gardner and T.J. Gray, Atomic Data and Nuclear Data Tables 21 (1978) 515.
9. P.H. Nettles et al., Proc. Intern. Conf. on Inner-Shell Ionization Phen. (Atlanta, 1972) p. 1420.
10. R. Rice, G. Basbas and F.D. McDaniel, Atomic Data and Nuclear Data Tables 20 (1977) 503.
11. G. Basbas, W. Brandt and R. Laubert, Phys. Rev. A17 (1978) 1655.
12. P.A. Amundsen, J. Phys. B9 (1976) 971.
13. R. Anholt, Phys. Rev. A17 (1978) 983.
14. K. Siwek-Wilczyńska et al., Nucl. Phys. A330 (1979) 150.
15. M. Blann, Univ. of Rochester Reports Nos. UR-NSRL-159 and COO-3494-34 (1977).
16. W. Broniowski, priv. communication.
17. J. Wilczyński et al., Phys. Rev. Letters 45 (1980) 606.